72nd International Astronautical Congress (IAC), Dubai, United Arab Emirates, 25-29 October 2021.

IAC-21-C1.3.9

Approaches to studying the performance of swarm decentralized control algorithms

Uliana Monahova[a]*, Danil Ivanov[b], Yaroslav Mashtakov[c], Sergey Shestakov[d]

[a] *Space Systems Dynamics Department, Keldysh Institute of Applied Mathematics, RAS, Moscow, Russian Federation, monakhova@phystech.edu*
[b] *Space Systems Dynamics Department, Keldysh Institute of Applied Mathematics, RAS, Moscow, Russian Federation, danilivanovs@gmail.com*
[c] *Space Systems Dynamics Department, Keldysh Institute of Applied Mathematics, RAS, Moscow, Russian Federation, yarmashtakov@gmail.com*
[d] *Space Systems Dynamics Department, Keldysh Institute of Applied Mathematics, RAS, Moscow, Russian Federation, shestakov.sa@gmail.com*

* Corresponding Author

Abstract

The problem of satellite swarm relative drift stopping is considered in the paper. The proposed decentralized control takes into account a communication constraint such as limited communication area, i.e. the maximum distance between the satellites. Only the satellites within communication area can be identified by relative motion determination system. The control algorithm aim is to eliminate the mean relative drift of all the satellites inside the communication area. The purpose of the work is to develop an approach, and to study the performance of the proposed decentralized control algorithm. The analytical study of the controlled system is performed. It is shown that the dynamical matrix of differential equations for the relative drift coincides with the Laplacian matrix of the communication graph. The eigenvalues of the system has one zero value and the rest negative values in case of the connected communication graph of the swarm. It means that all the relative drifts converge to the same value under the proposed control. The speed of convergence is defined by the maximal negative eigenvalue that depend on the graph topology. The initial drift and the convergence speed make it possible to estimate the communication distance for different topologies to provide the connectivity of the graph. The shortcoming of this estimation is that the graph is dynamically changing during the convergence. The different approach is to assume that after the launch, the relative distances are small and the graph is complete. Considering the initial velocity normally distributed errors, it is possible to estimate the distance between any two satellites after the convergence. It provides an estimation on the communication distance to ensure the relative drift elimination between all the satellites in the swarm. The resulted estimations are validated using Monte Carlo simulations of the controlled motion after the launch with dynamical communication graph.

Keywords: swarm of satellites, decentralized control, relative drift

1. Introduction

A swarm is a type of satellite formation involving a large number of satellites that typically requires only bounded relative motion with no other restrictions. The advantages of random relative trajectories in the swarm are reduced dependence on the failure of the specific satellite and soft demands for the on-board hardware and software. The deployment of distributed systems implies some difficulties caused by the errors in the initial conditions after the separation from the launch vehicle. This leads to a slightly different orbital period of the satellites, so the relative trajectories become unlimited and the swarm degrades. Space systems consisting of numerous satellites often require decentralized relative motion control algorithms which are also characterized by some implementation errors. The decentralized control performance depends on the size of the satellite's communication area and on the number of the communicating satellites which relative motion is taken into account for control calculation. All these factors may cause the separation of some satellites from the swarm.

A number of control algorithms for the swarm using different control approaches has been proposed in literature. The common approach is to include a 3-axis propulsion system onboard, allowing unrestricted thrust direction. If the number of thrusters is limited, and thrust direction cannot be arbitrarily changed, a single-input control approach is also feasible, assuming the thrust vector is fixed in the body reference frame [1].

Miniaturized satellites have unavoidable constraints on size, mass, energy, and therefore conventional propulsion systems can hardly be used for relative motion control. Moreover, the thruster plumes can negatively affect neighbour satellites, "blinding" optical or thermal instruments onboard. Alternative approaches have been proposed in recent years to develop effective, self-sufficient methods for motion control without propellant consumption: using aerodynamic drag force and solar radiation pressure. Both methods require sails onboard or satellite specific form-factors with high area-to-mass ratios [2–7]. The principal idea is to use a difference in environmental forces acting on each satellite in the formation. Satellites connected by tethers also do not require any fuel, the relative motion is controlled by varying tether length [8–11], though the realization of this concept is complicated because of flexible tether motion [12]. Another approach is to use electrostatic force for formation flying control [13]. This concept is based on the SCATCHA mission [14] where the satellite electrostatic charge system was tested. The following papers [15–24] developed this idea.

In this paper the control method is based on the relative drift elimination algorithm developed by the authors in [4]. Its aim is to eliminate mean relative drift between the satellites in the communication area. In [4] it is achieved by the difference in the aerodynamic drag force applied in along-track direction. The proposed control was studied numerically and the range of system parameters when the control successfully achieves the near zero drift is estimated. However, in some cases some of the satellites separate from the group and the swarm become divided. Therefore, the purpose of this work is to study the performance of swarm control algorithm, and to develop simple estimation of the necessary size of communication area which guarantees convergence of the relative motion under given launch errors. The results obtained by the Monte Carlo method are compared with the developed estimations.

2. Problem Statement

Consider a significant number N of homogenous satellites launched in LEO. Each satellite is equipped with a relative motion determination system able to estimate the position and velocity of any neighbour satellite within the maximum range R_{comm}, which further will be referred as communication radius. If the distance to some satellite is more than R_{comm} – no information about its motion is available. The satellites are capable to produce a control force in the along-track direction either by the on-board propulsion or by some of the fuel-less approaches such as the difference in the aerodynamic drag, electromagnetic interaction, Lorenz force, etc. Each satellite applies the decentralized control algorithm in order to stop the relative drift between all the satellites within the communication area.

In the paper two approaches are proposed. First, analytical approach based on the fixed communication topology allows estimating the convergence time for the controlled motion. It allows to preliminary calculate the worst case for the system. The second approach is to assume the complete initial graph and estimate the required communication radius demanding the complete graph after the convergence. It provides the optimistic scenario. The two estimations can be verified by the numerical simulations of the swarm controlled motion.

2.1 Motion equations

For algorithm performance investigation, the relative motion equations are required. The Hill-Clohessy-Wiltshire (HCW) equations are utilized to describe the relative motion of two arbitrarily chosen satellites within the swarm [25], in a leader-follower system expressed in the rotating Local-Vertical-Local-Horizontal reference frame (LVLH) designated as $Oxyz$. Its origin is located at a reference point moving along a circular orbit with radius r_0, at an orbital angular velocity ω. The *z*-axis points towards the radial direction, the *y*-axis is aligned with orbital momentum and the *x*-axis completes the right-handed orthogonal frame. These linearized ordinary differential equations of free motion can be solved analytically. The equations are valid for small relative distances, therefore the relative distance between the leader and follower must be several orders of magnitude smaller than the orbital radius.

Let $\mathbf{r}_i = \left[x_i, y_i, z_i\right]^T$ and $\mathbf{r}_j = \left[x_j, y_j, z_j\right]^T$ be the vectors of the *i*-th and *j*-th satellites in the LVLH reference frame, $i \neq j, i = 1,...,N, j = 1,...,N,$ where N is the number of the satellites in the swarm. Then the components of the relative position vector $\mathbf{r}_{ij} = \mathbf{r}_j - \mathbf{r}_i = \left[x_{ij}, y_{ij}, z_{ij}\right]^T$ can be described by following equations:

$$\begin{aligned} &\ddot{x}_{ij} + 2\omega\dot{z}_{ij} = 0, \\ &\ddot{y}_{ij} + \omega^2 y_{ij} = 0, \\ &\ddot{z}_{ij} - 2\omega\dot{x}_{ij} - 3\omega^2 z_{ij} = 0, \end{aligned} \tag{1}$$

The solution can be written as follows:

$$\begin{aligned} x_{ij} &= D_{ij} + 2A_{ij}\cos\left(\omega t + \psi_{ij}\right), \\ y_{ij} &= B_{ij}\cos\left(\omega t + \varphi_{ij}\right), \\ z_{ij} &= 2C_{ij} + A_{ij}\sin\left(\omega t + \psi_{ij}\right), \end{aligned} \tag{2}$$

where $A, B, C, D, \psi, \varphi$ are the motion parameters that depend on initial conditions:

$$C_{ij} = \frac{\dot{x}_{ij}(0)}{\omega} + 2z_{ij}(0)$$
$$D_{ij}(t) = -3C_{ij}\omega t + x_{ij}(0) - \frac{2\dot{z}_{ij}(0)}{\omega}$$
$$B_{ij} = \sqrt{\frac{\dot{y}_{ij}^2(0)}{\omega^2} + y_{ij}^2(0)} \quad (3)$$
$$A_{ij} = \frac{1}{\omega}\sqrt{\dot{z}_{ij}^2(0) + 4z_{ij}^2(0)\omega^2 + 8z_{ij}(0)\dot{x}_{ij}(0)\omega + 4\dot{x}_{ij}^2(0)}$$

Consider the controlled motion equations of the swarm, and assume that the *i*-th satellite is equipped with a motion control system able to produce the acceleration $\mathbf{u}_i$. In this case the parameters $A, B, C, D, \psi, \varphi$ are determined by following differential equations:

$$\begin{aligned}
\dot{A}_{ij} &= \frac{1}{\omega}\left(u_{ij}^z \cos\psi_{ij} - 2u_{ij}^x \sin\psi_{ij}\right),\\
\dot{B}_{ij} &= -\frac{1}{\omega}u_{ij}^y \sin\varphi_{ij},\\
\dot{C}_{ij} &= \frac{1}{\omega}u_{ij}^x,\\
\dot{D}_{ij} &= -3\omega C_{ij} - \frac{2}{\omega}u_{ij}^z,\\
\dot{\psi}_{ij} &= -\frac{1}{\omega A_{ij}}\left(u_{ij}^z \sin\psi_{ij} + 2u_{ij}^x \cos\psi_{ij}\right),\\
\dot{\varphi}_{ij} &= -\frac{1}{\omega B_{ij}}u_{ij}^y \sin\varphi_{ij},
\end{aligned} \quad (4)$$

where $\left[u_{ij}^x, u_{ij}^y, u_{ij}^z\right]^T$ are components of acceleration difference $\mathbf{u}_j - \mathbf{u}_i$ between *i*-th and *j*-th satellite. In this work the acceleration only along *Ox* axis is considered. Parameters C_{ij} are responsible for the relative drift and are of special interest in our work.

2.2 Decentralized control algorithm

In this work the decentralized control for relative drift elimination based on the mean drift parameter value is considered. If for the *i*-th satellite there are N_{comm} satellites with known relative motion, then the average constant $\bar{C}_i$ is equal to:

$$\bar{C}_i = \sum_{j=1}^{N_{comm}} C_{ij} / N_{comm}. \quad (5)$$

The corresponding control applied to the satellite has the form:

$$\bar{u}_i = -k\,\bar{C}_i. \quad (6)$$

where $k > 0$ is the control parameter.

2.3 Launch conditions

Consider the application of the proposed control rules for the task of the swarm of nanosatellites construction after the launch. It is assumed that the satellites separate from the bus-launcher in the *Ox* axis direction one after another with the time interval Δt between the launches. The velocity of the ejection is the same for all the CubeSats, however due to launch system inaccuracy the ejection velocity $\mathbf{V}_0$ is subjected to errors. So, the initial velocity vector $\mathbf{V}_0$ in orbital reference frame is modelled as $\mathbf{V}_0 = \left[V_e, 0, 0\right]^T$, where $\mathbf{V}_0$ is normally distributed random value with expected value $E\left[\mathbf{V}_0\right] = \left[V_e, 0, 0\right]^T$ and variance $\mathrm{Var}\left[\mathbf{V}_0\right] = \left[\sigma_V, \sigma_V, \sigma_V\right]^T$.

3. Communication graph and convergence rate

3.1 Graph theory preliminaries

The term graph will refer to a simple undirected unweighted graph $G = (V, E)$, where V is the set of vertices, E is the set of edges. Every edge connects two distinct vertices; every pair of vertices is connected by at most one edge.

If every pair of vertices is connected by exactly one edge, G is called complete.

An adjacency matrix $\hat{A}$ of a graph G on N vertices is a $N \times N$ matrix such that the element in *i*-th row and *j*-th column is one when there is an edge between vertex *i* and vertex *j*, and zero when there is no such edge.

A degree of a vertex v is the number of vertices adjacent to v. A degree matrix $\hat{D}$ is a diagonal $N \times N$ matrix with diagonal elements being the degrees of individual vertices.

A path between vertices *i* and *j* in a graph is a sequence of edges which joins these two vertices. The graph is called connected if there is a path between any two vertices. The length of a path is the number of edges in it. The diameter of a connected graph is the greatest distance between any pair of vertices.

3.2 Laplacian matrix eigenvalues estimations

The control equations presented above allow reformulating the problem in terms of graph theory. We associate a graph to a given swarm. The vertices of the underlying graph are the satellites. The edge between vertices number *i* and *j* exists if *i*-th and *j*-th satellites "see" each other, i.e. the distance between them is less than the communication radius R_{comm}. Within such an interpretation the complete graph on N vertices corresponds to a swarm of N satellites, where every satellite can communicate with every other one.

According to equations presented above swarm control is determined by relative drifts C_{ij}. Assuming C_i is the drift of the *i*-th satellite with respect to LVLH reference frame relative drifts are $C_{ij} = C_i - C_j$.

The average controlled drift $\bar{C}_i$ depends on individual drifts C_i in a following way. For *i*-th satellite: $N_{comm}{}^i$ satellites contribute to average drift, $N - N_{comm}^i - 1$ do not affect the control in any way, the remaining one is the *i*-th satellite itself.

Let matrix $\hat{S}$ be a matrix of size $N \times N$ where

$$s_{ij} = \begin{cases} 1 & \text{if } i = j \\ 0 & \text{if } i \neq j \text{ and sat } i \text{ does not see sat } j \\ -1/N_{comm}^i & \text{if } i \neq j \text{ and sat } i \text{ sees sat } j \end{cases}$$

Then $\bar{C} = \hat{S}C$, where $\bar{C}$ and C are column vectors of corresponding drifts.

For a graph G with adjacency matrix $\hat{A}$ and degree matrix $\hat{D}$ the Laplacian matrix (or sometimes Kirchhoff matrix or admittance matrix) is defined as $\hat{L} = \hat{D} - \hat{A}$ [26,27]. The normalized Laplacian matrix is defined as $\mathcal{L} = \hat{D}^{-1/2}\hat{L}\hat{D}^{-1/2}$ [26]. While matrix $\hat{S}$ is not equal to any of aforementioned matrices, $\hat{S}$ is similar to $\mathcal{L}$ via

$$\hat{S} = \hat{D}^{-1/2}\mathcal{L}\hat{D}^{1/2} \tag{7}$$

so the spectra of $\hat{S}$ and $\mathcal{L}$ coincide. The spectrum of $\mathcal{L}$ is an important property of the underlying graph G. In our control algorithm two properties of spectrum are of the most importance [26].

1) Zero is always an eigenvalue. The multiplicity of zero in the spectrum is equal to the number of connected component of a graph G.
2) All nonzero eigenvalues are strictly positive.

That means, that if a graph is connected i.e. the satellites of the swarm are forming one connected group, then the control always nullifies relative drift. One-dimensional null-vector subspace corresponds to the drift of the whole swarm as a group.

Moreover, as differential equations of the control are first-order linear, the relative drift exponentially decreases to zero. The smallest positive eigenvalue λ_1 corresponds to the speed of such a decrease (the least of all the exponent powers).

For general connected graph G it is difficult to analytically calculate convergence rate λ_1, nevertheless the following is true.

1) For a complete graph on n vertices $\lambda_1 = \dfrac{n}{n-1}$ [26]
2) For a general graph on n vertices with maximal vertex degree d_{max} and diameter Δ $\lambda_1 \geq \dfrac{4}{n\Delta d_{max}}$ [28,29]

It is necessary to emphasize that the lower bound is not tight and in fact is very bad for general graphs, so typically the speed of drift convergence due to the presented control would be much higher.

4. Dependence of communication radius on the launch parameters

Due to the considered launch scheme from the carrier rocket, it can be seen from the motion equations (2) that parameter D_{ij} mainly affects the divergence of the swarm. Thus, to determine the radius of communication sphere necessary to maintain the connectivity of the swarm, D_{ij} needs to be estimated. This parameter is random variable, therefore only its expected value and variance can be found. In view of the fact that mission consists of two phases: the launch and the controlled motion, the expected value $E\left[D_{ij}\right]$ and variance $\mathrm{Var}\left[D_{ij}\right]$ after the launch will be estimated first. Using equations (3), the value of parameters D_1, D_2 for the first two launched satellites at the end of the first phase can be found:

$$\begin{aligned} D_1(T) &= -3C_1(t_0)\omega N\Delta t + D_1(t_0), \\ D_2(T) &= -3C_2(t_0)\omega(N-1)\Delta t + D_2(t_0), \end{aligned} \tag{8}$$

where T is the time when the last satellite is launched, $C_1(t_0)$, $C_2(t_0)$ are the initial drift values of first and second launched satellites respectively, Δt is the time interval between launches, $D_1(t_0)$, $D_2(t_0)$ are the initial values of parameters D_1, D_2. Now, taking into account that the initial values of D^1, D^2, C^1, C^2 are independent random variables, $\mathrm{Var}\left[D_{21}(T)\right]$ and $E\left[D_{21}(T)\right]$ can be calculated:

$$\begin{aligned} &\mathrm{Var}\left[D_{21}(T)\right] = \mathrm{Var}\left[D_2(T) - D_1(T)\right] \\ &= 9\omega^2\Delta t^2(N-1)^2\,\mathrm{Var}\left[C_2(t_0)\right] + \mathrm{Var}\left[D_2(t_0)\right] \\ &+9\omega^2\Delta t^2 N^2\,\mathrm{Var}\left[C_1(t_0)\right] + \mathrm{Var}\left[D_1(t_0)\right], \end{aligned} \tag{9}$$

$$\begin{aligned} &E\left[D_{21}(T)\right] = E\left[D_2(T) - D_1(T)\right] \\ &= -3\omega(N-1)\Delta t E\left[C_2(t_0)\right] + 3\omega N\Delta t E\left[C_1(t_0)\right] \\ &+E\left[D_2(t_0)\right] - E\left[D_1(t_0)\right]. \end{aligned} \tag{10}$$

Substituting equations (3) and considering errors only in ejection velocities,

$$\begin{aligned}\mathrm{Var}\left[D_{21}(T)\right] &= 9\omega^2\Delta t^2 N^2\,\mathrm{Var}\left[\frac{\dot{x}_1(t_0)}{\omega}\right] \\ &+9\omega^2\Delta t^2(N-1)^2\,\mathrm{Var}\left[\frac{\dot{x}_2(t_0)}{\omega}\right] \\ &+\mathrm{Var}\left[\frac{2\dot{z}_1(t_0)}{\omega}\right]+\mathrm{Var}\left[\frac{2\dot{z}_2(t_0)}{\omega}\right] \\ &= 9\omega^2\Delta t^2\left(N^2\frac{\sigma_V^2}{\omega^2}+(N-1)^2\frac{\sigma_V^2}{\omega^2}\right)+\frac{8\sigma_V^2}{\omega^2} \\ &= \sigma_V^2\left(9\Delta t^2(2N^2-2N+1)+\frac{8}{\omega^2}\right),\end{aligned} \tag{11}$$

$$\begin{aligned}E\left[D_{21}(T)\right] &= -3\omega(N-1)\Delta t E\left[\frac{\dot{x}_2(t_0)}{\omega}\right] \\ &+3\omega N\Delta t E\left[\frac{\dot{x}_1(t_0)}{\omega}\right]+E\left[\frac{2\dot{z}_2(t_0)}{\omega}\right]-E\left[\frac{2\dot{z}_1(t_0)}{\omega}\right] \\ &= 3\Delta t\,\mu_V,\end{aligned} \tag{12}$$

where σ_V, μ_V are standard deviation and expected value of ejection velocities accordingly. First two launched satellites were chosen to calculate expected value and variance because they have the biggest $\mathrm{Var}\left[D_{ij}\right]$ between satellites.

The next step is to estimate $E\left[D_{21}\right]$ and $\mathrm{Var}\left[D_{21}\right]$ at the end of the second phase. Using equations (4), the value of parameters D_1, D_2 for the first two launched satellites at the end of the controlled motion can be found:

$$\begin{aligned}&D_2(T_{end})-D_1(T_{end}) = D_2(T)-D_1(T) \\ &-3\omega\int C_2(t)dt+3\omega\int C_1(t)dt \\ &= D_2(T)-D_1(T)+(b_1-b_2)3\omega\int e^{-\lambda_1 t}dt,\end{aligned} \tag{13}$$

where T_{end} is the time when the second phase ends, b_1, b_2 are coefficients defined by initial C_1, C_2. Estimating the integral at the limit to infinity:

$$D_{21}(T_{end}) = D_2(T)-D_1(T)+(b_1-b_2)3\omega\frac{1}{\lambda_1}. \tag{14}$$

The $\mathrm{Var}\left[D_{21}(T_{end})\right]$ and $E\left[D_{21}(T_{end})\right]$ can be calculated as:

$$\begin{aligned}\mathrm{Var}\left[D_{21}(T_{end})\right] &= \mathrm{Var}\left[D_2(T)-D_1(T)\right] \\ &+\mathrm{Var}\left[(b_1-b_2)3\omega\frac{1}{\lambda_1}\right] \\ &= \sigma_V^2\left(9\Delta t^2(2N^2-2N+1)+\frac{8}{\omega^2}\right)+18\omega^2\frac{1}{\lambda_1^2}\frac{\sigma_V^2}{\omega^2} \\ &= \sigma_V^2\left(9\Delta t^2(2N^2-2N+1)+\frac{8}{\omega^2}+\frac{18}{\lambda_1^2}\right),\end{aligned} \tag{15}$$

$$\begin{aligned}E\left[D_{21}(T_{end})\right] &= E\left[D_2(T)-D_1(T)\right] \\ &+E\left[(b_1-b_2)3\omega\frac{1}{\lambda_1}\right] = 3\Delta t\,\mu_V.\end{aligned} \tag{16}$$

Introducing new designations $\mu_D = E\left[D_{21}(T_{end})\right]$ and $\sigma_D = \sqrt{\mathrm{Var}\left[D_{21}(T_{end})\right]}$, we can estimate required radius of communication sphere R_{comm} for two neighbouring satellites to be connected:

$$\begin{aligned}R_{comm} &= \mu_D+3\sigma_D \\ &= 3\Delta t\,\mu_V+3\sigma_V\sqrt{9\Delta t^2(2N^2-2N+1)+\frac{8}{\omega^2}+\frac{18}{\lambda_1^2}}.\end{aligned} \tag{17}$$

5. Numerical investigation and verification

5.1 Parameters of the simulations

Consider the application of the proposed control algorithms and strategies for the problem of the nanosatellites swarm construction after the launch. All parameters used in the simulation of the controlled motion of the swarm are presented in Table 1.

Table 1. Simulation parameters

Main parameters of the swarm	
Number of satellites in the swarm, N	20
Mass of satellite, m	3 kg
Initial conditions	
Ejection velocity, V_e	0.05 m/s
Deviation of ejection velocity, σ_V	0.01 m/s
Time interval between ejections, Δt	3 s
Orbital parameters	
Orbit altitude, h	500 km
Orbit inclination, i	51.7^o
Algorithms parameters	
Time interval between control calculation	600 s
Control coefficient, k	$1.85\cdot10^{-7}$

Since the motion along the Oy axis is uncontrolled, the trajectories in figures are displayed further in projection on Oxz plane.

5.2 Example of the successful drift elimination

Consider the application of average drift elimination control law to the swarm construction problem. The control begins after the launching of all satellites. The average drift elimination control (6) is calculated every 600 s taking into account restrictions implied on radius of communication sphere. For initial conditions presented at Table 1 the R_{comm} is 730 m according to (17). Fig. 1 shows the controlled relative motion

trajectories, which after a while become closed. Thus, the swarm of satellites is constructed. The drifts C_{ij} relative to the first ejected satellite are shown in Fig. 2. The relative drifts converge to zero which confirms that in Fig.1 relative trajectories of the satellites in the swarm become closed. One can see that the swarm is constructed in 7 hours.

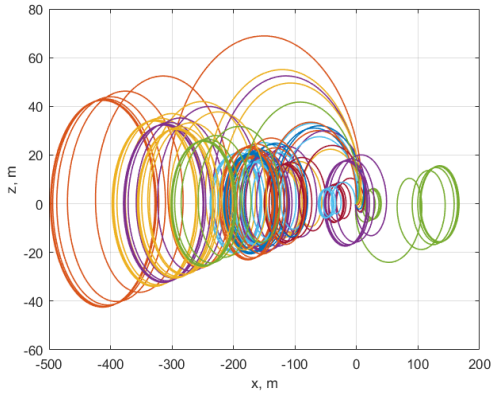

Fig. 1. Relative trajectories under proposed control in case when $R_{comm} = \mu_D + 3\sigma_D$

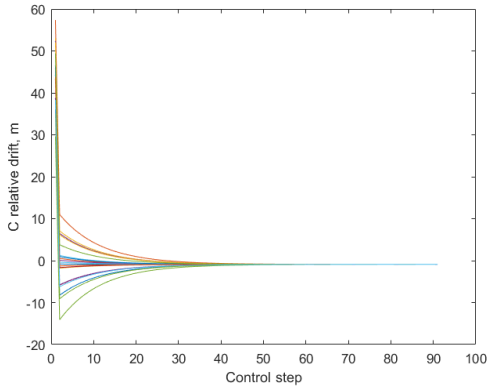

Fig. 2. Relative drifts

Fig. 3 shows the applied control for all satellites. The control coefficient was chosen so that control did not exceed the feasible values of aerodynamic force. Initially the calculated control is maximum for almost all satellites, and it decreases as the relative drift converges to a zero. Fig. 4 demonstrates D_{ij} parameters relative to the first ejected satellite. These parameters become constant, since relative drift converges to zero.

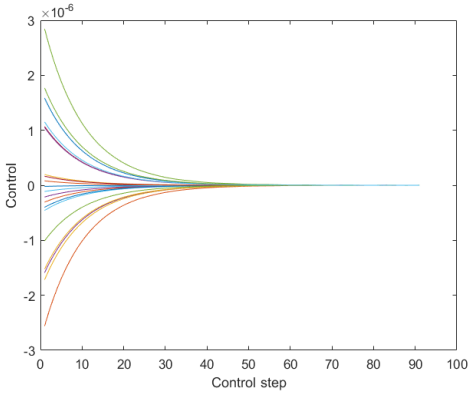

Fig. 3. Required control

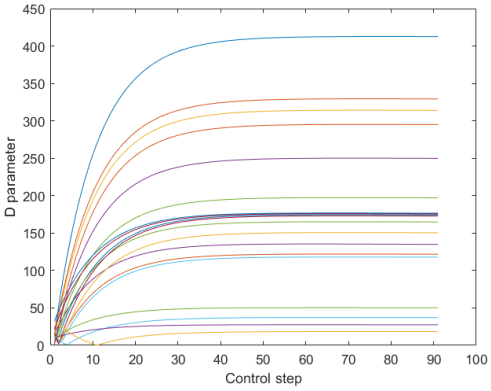

Fig. 4. D_i parameter

5.3 Swarm separation example

In this section the example of swarm separation is considered. The initial conditions are the same as in the presented earlier simulation. The difference will be only in restrictions implied on radius of communication sphere. For this simulation R_{comm} is counted as $\mu_D + 0.5\sigma_D$ that is 122 m. The relative trajectories of the satellites are shown in Fig. 5. One can see that satellites are separating from each other.

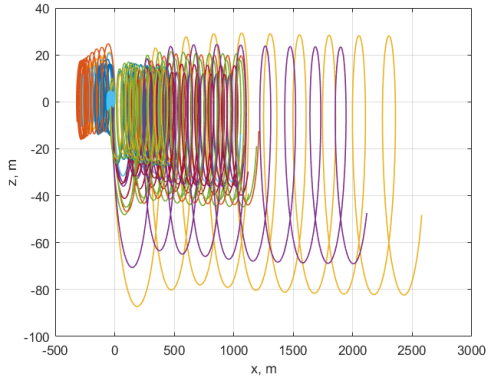

Fig. 5. Relative trajectories under proposed control in case when $R_{comm} = \mu_D + 0.5\sigma_D$

Fig. 6 demonstrates the drifts C_{ij} relative to the first ejected satellite and it can be seen that relative drifts cannot converge to zero. This happens because the value of R_{comm} was chosen small and satellites can analyze motion only of few satellites in the group. In addition, Fig. 6 shows that satellites divided into five independent groups and had similar values of drift inside them. The D_{ij} parameters relative to the first ejected satellite are shown at Fig. 7. In the contrary to previous simulation, D_{ij} parameters increase in time and do not converge to constant values.

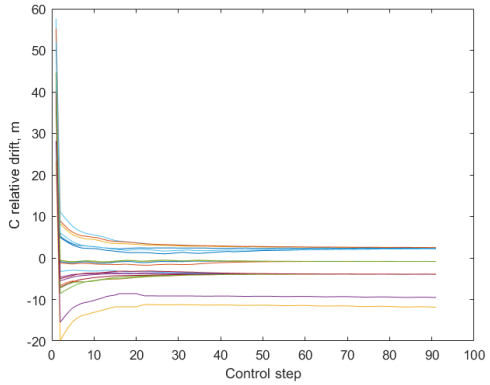

Fig. 6. Relative drifts

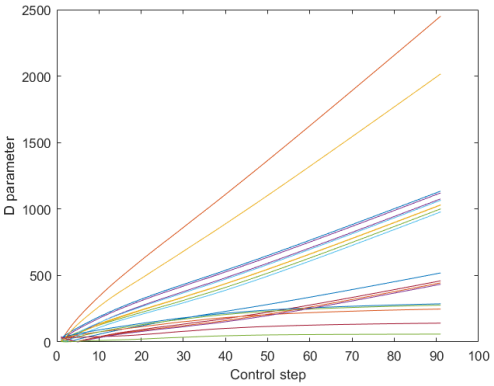

Fig. 7. D_i parameter

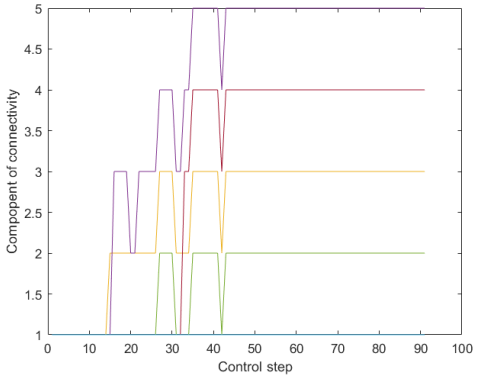

Fig. 8. Connectivity component of graph

Fig. 8 shows component of connectivity of the graph. During first 15 control steps, the group of satellites formed connected graph because component of connectivity was one. After the 15th step the graph became disconnected and had component of connectivity equal to five. This also confirms that satellites divided into five independent groups.

5.4 Monte Carlo simulations

The dependence of the swarm separation effect on the communication sphere radius is of particular interest and should be investigated. Since the considered ejection velocity errors are random values then the results of the swarm construction are also random. Let us investigate the performance of control laws using multiple numerical simulations with various parameters. A series of identical numerical experiments with fixed set of parameters, except the R_{comm}, is performed. After each simulation the relative drifts convergence to zero is checked. It is possible that at the end of the simulation the satellites in the swarm will form several clusters, or subgroups, such that inside one cluster relative drifts are close to zero. If the swarm is divided, the number of satellites in each subgroup with the same relative drifts is calculated. Denote the amount of satellites in the biggest subgroup as $N_{cluster}$. The effect of the swarm separation is measured as $N_{cluster} / N_{total}$. If $N_{cluster} / N_{total} = 1$ then there is no satellite that is separated from the swarm. If this ratio is close to 1, this corresponds to the case when a small number of satellites leave the swarm but the majority remain in the same group. Other cases refer to the separation of the group into many independent subgroups.

For each value of R_{comm} (e.g. $R_{comm} = \mu_D + 0.75\sigma_D$) 200 simulation were carried out. For each simulation a ratio $N_{cluster} / N_{total}$ and number of subgroups are calculated. The results of these numerous simulations are presented in Fig. 10 and Fig. 11. The *x* axis in these figures corresponds to the α in $R_{comm} = \mu_D + \alpha \cdot \sigma_D$. When $R_{comm} = \mu_D + 3\sigma_D$ it can be seen that satellites form one group in all 200 simulations. It means that our numerical results corresponds to analytical estimation (17) of R_{comm} necessary to maintain connectivity of the swarm. Also, with decrease of α, the connectivity of the swarm decreases.

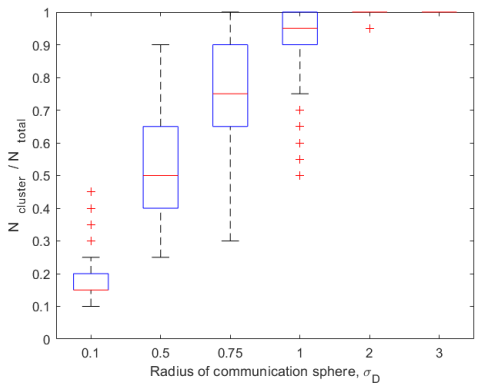

Fig. 10. Percentage of satellites aligned the drift depending on the value of R_{comm}

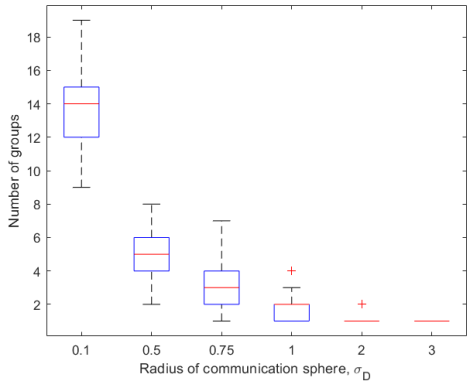

Fig. 11. Number of groups in the swarm depending on the value of R_{comm}

6. Conclusions

Application of decentralized control based on the motion of satellites inside the communication sphere makes it possible to construct a swarm of satellites after the launch. However, it is necessary to take into account the communication constraints caused by the features of the relative motion determination system and/or inter-satellite communication. The swarm separation effect is studied numerically depending on different values of R_{comm}. Our analytical estimations of R_{comm} necessary to maintain connectivity of the swarm was supported by numerical results obtained in Monte Carlo simulations.

Acknowledgements

The work is supported by the Russian Science Foundation, grant № 17-71-20117.

References

1. Guerman, A.; Ovchinnikov, M.; Smirnov, G.; Trofimov, S. Closed Relative Trajectories for Formation Flying with Single-Input Control. *Math. Probl. Eng.* **2012**, *2012*, 1–20, doi:10.1155/2012/967248.
2. Gong, S.; Yunfeng, G.; Li, J. Solar sail formation flying on an inclined Earth orbit. *Acta Astronaut.* **2011**, *68*, 226–239, doi:10.1016/j.actaastro.2010.08.022.
3. Shengping, G.; Hexi, B.; Junfeng, L. Solar sail formation flying around displaced solar orbits. *J. Guid. Control. Dyn.* **2007**, *30*, 1148–1152, doi:10.2514/1.24315.
4. Ivanov, D.; Monakhova, U.; Ovchinnikov, M. Nanosatellites swarm deployment using decentralized differential drag-based control with communicational constraints. *Acta Astronaut.* **2019**, *159*, 646–657, doi:10.1016/J.ACTAASTRO.2019.02.006.
5. Ivanov, D.; Monakhova, U.; Guerman, A.; Ovchinnikov, M.; Roldugin, D. Decentralized differential drag based control of nanosatellites swarm spatial distribution using magnetorquers. *Adv. Sp. Res.* **2021**, *67*, 3489–3503, doi:10.1016/j.asr.2020.05.024.
6. Ivanov, D.; Kushniruk, M.; Ovchinnikov, M. Study of satellite formation flying control using differential lift and drag. *Acta Astronaut.* **2018**, *145*, 88–100, doi:10.1016/J.ACTAASTRO.2018.07.047.
7. Mashtakov, Y.; Ovchinnikov, M.; Petrova, T.; Tkachev, S. Two-satellite formation flying control by cell-structured solar sail. *Acta Astronaut.* **2020**, *170*, 592–600, doi:10.1016/j.actaastro.2020.02.024.
8. Chung, S.-J.; Miller, D.W. Propellant-Free Control of Tethered Formation Flight, Part 1: Linear Control and Experimentation. *J. Guid. Control. Dyn.* **2008**, *31*, 571–584, doi:10.2514/1.32188.
9. Zhang, J.; Yang, K.; Qi, R. Dynamics and offset control of tethered space-tug system. *Acta Astronaut.* **2018**, *142*, 232–252, doi:10.1016/J.ACTAASTRO.2017.10.020.
10. Chen, Y.; Huang, R.; Ren, X.; He, L.; He, Y. History of the Tether Concept and Tether Missions: A Review. *ISRN Astron. Astrophys.* **2013**, *2013*, 1–7, doi:10.1155/2013/502973.
11. Guerman, A.D.; Smirnov, G.; Paglione, P.; Vale Seabra, A.M. Stationary Configurations of a Tetrahedral Tethered Satellite Formation. *J. Guid. Control. Dyn.* **2008**, *31*, 424–428, doi:10.2514/1.31979.
12. Gates, S.S.; Koss, S.M.; Zedd, M.F. Advanced Tether Experiment Deployment Failure. *J. Spacecr. Rockets* **2001**, *38*, 60–68.
13. King, L.B.; Parker, G.G. Spacecraft Formation-flying using Inter-vehicle Coulomb Forces. **2002**, 1–103.
14. Mullen, E.G.; Gussenhoven, M.S.; Hardy, D.A. SCATHA Survey of High-Voltage Spacecraft Charging in Sunlight. *J. Geophys. Sci.* **1986**, *91*, 1074–1090.
15. Felicetti, L.; Palmerini, G.B. Analytical and numerical investigations on spacecraft formation control by using electrostatic forces. *Acta Astronaut.* **2016**, *123*, 455–469, doi:10.1016/j.actaastro.2015.12.056.
16. Felicetti, L.; Palmerini, G.B. Three spacecraft formation control by means of electrostatic forces. *Aerosp. Sci. Technol.* **2016**, *48*, 261–271, doi:10.1016/j.ast.2015.11.022.
17. Inampudi, R.; Schaub, H. Optimal Reconfigurations of Two-Craft Coulomb Formation in Circular Orbits. *Proc. AIAA Guid. Navig. Control Conf.* **2010**, *35*, doi:10.2514/1.56551.
18. Saaj, C.M.; Lappas, V.; Schaub, H.; Izzo, D. Hybrid propulsion system for formation flying using electrostatic forces. *Aerosp. Sci. Technol.* **2010**, *14*, 348–355, doi:10.1016/j.ast.2010.02.009.
19. Hogan, E.A.; Schaub, H. Collinear invariant shapes for three-spacecraft Coulomb formations. *Acta Astronaut.* **2012**, *72*, 78–89, doi:10.1016/j.actaastro.2011.10.020.
20. Inampudi, R.; Schaub, H. Orbit Radial Dynamic Analysis of Two-Craft Coulomb Formation at Libration Points. *J. Guid. Control. Dyn.* **2014**, *37*, 682–691, doi:10.2514/1.55282.
21. Hogan, E.A.; Schaub, H. Relative motion control for two-spacecraft electrostatic orbit corrections. *Adv. Astronaut. Sci.* **2012**, *142*, 967–986, doi:10.2514/1.56118.

22. Schaub, H.; Jasper, L.E.Z. Orbit Boosting Maneuvers for Two-Craft Coulomb Formations. *J. Guid. Control. Dyn.* **2013**, *36*, 74–82, doi:10.2514/1.57479.
23. Jasch, P.D.; Hogan, E.A.; Schaub, H. Stability analysis and out-of-plane control of collinear spinning three-craft Coulomb formations. *Adv. Astronaut. Sci.* **2012**, *143*, 747–762, doi:10.1016/j.actaastro.2013.03.005.
24. Jones, D.R.; Schaub, H. Collinear Three-Craft Coulomb Formation Stability Analysis and Control. *J. Guid. Control. Dyn.* **2014**, *37*, 224–232, doi:10.2514/1.60293.
25. Hill G.W. Researches in Lunar Theory. *Am. J. Math.* **1878**, *1*, 5–26.
26. Chung, F.R.K. Lectures on Spectral Graph Theory. *Lect. Notes* 2001.
27. Cvetković, D.M.; Doob, M.; Sachs, H. *Spectra of Graphs: Theory and Application*; Pure and applied mathematics : a series of monographs and textbooks; Academic Press, 1980; ISBN 9780121951504.
28. Mohar, B. Eigenvalues, diameter, and mean distance in graphs. *Graphs Comb.* **1991**, doi:10.1007/BF01789463.
29. Butler, S. Eigenvalues and structures of graphs. *Ph.D. Diss.* **2008**, 89.